Proper Orthogonal Decomposition Analysis of Cross Sectional Fuel Spray Data

Santosh Tirunagari*, Tuomo Hulkkonen, Ville Vuorinen, Ossi Kaario, Martti Larmi
Aalto University, School of Engineering, Espoo, Finland
(santosh.tirunagari, tuomo.hulkkonen, ville.vuorinen, ossi.kaario, martti.larmi)@aalto.fi

Abstract

In the present study, we analyse laser sheet spray imaging data using Proper Orthogonal Decomposition (POD). The analysis sheds light into the spray structures including spray-vortex interaction. The analysis of these structures is essential in understanding the fundamentals of spray characteristics. We study the influence of injection pressure on spray formation. Two different cases are considered corresponding to 450 bar, and 1000 bar injection pressures. The POD analysis reveals that the spray images can be decomposed into a set of orthogonal basis functions which provide more insight to the structures seen by bare eye. The effect of injection pressure is coherently explained with the POD modes. In particular, with the increase in pressure, might lead to better mixing in sprays. Furthermore, the sensitivity analysis of the POD modes reveals that the present conclusions are independent of the number of spray images for considered ensembles.

Introduction

Today one of the major problems of oil based energy and transport sectors is exhaust gas emissions. Researchers are searching for ways to reduce the emission. The emissions of modern diesel engines are mainly related to NOx and soot. The origin of soot emissions are in fuel rich combustion conditions that are a result of poor mixing between fuel droplets and the surrounding air. The turbulent mixing of fuel droplets in engines is crucial in determining the amount of soot produced by the spray combustion process [1]. Therefore the understanding and research concerning fuel spray mixing is very important.

To gain a deeper understanding on combustion process and turbulent fuel air mixing, machine-learning methods can be utilised. This field allows computers to adopt behaviors based on training data. These methods recognize complex patterns and makes intelligent decisions based on data [2]. These techniques include: reduced order models or dimensionality reduction methods, statistical, and machine vision methods. Dimensionality reduction is a technique used to find a reduced order model on a given data. Such a technique includes feature selection and feature extraction methods. Feature selection is based on selecting a subset of variables which best define the data, whereas feature extraction transforms the data from high-dimensional space to a space of fewer dimensions [2]. The data transformation may be linear, as in Proper Orthogonal Decomposition (POD).

Proper Orthogonal Decomposition (POD) can be used to analyze the spray formation and to shed further light into understanding the fundamentals of spray characteristics such as spray-vortex interactions. From the literature, it is expected that POD would be a good method for analyzing the flow structures. For example, Perrin et. al [3] used POD to obtain phase averaged turbulence properties for flow past a cylinder. In highly turbulent flows, the coherent flow structures are difficult to identify due to the combination of organized and chaotic fluctuating motions. Using POD analysis it is shown in [3], that von Karman vortices can be reproduced within the first few modes. POD has also been used as a tool for the comparison of Particle Image Velocimetry (PIV) and Large Eddy Simulation (LES) data in [4] and it is also shown that POD modes have a good qualitative agreement between PIV and LES. POD was applied to the image sequence prior to image analysis in [5]. The reconstruction of a snapshot using POD analysis observed reduction of droplet noise in the spray boundaries, resulting in a smoother boundary for edge detection. This analysis processed the morphological parameters including spray boundary, widths, and angles of ill-behaved sprays.

The POD modes can be considered to be energetically the optimal decomposition for the flow. Only a few POD modes are required to capture the large scale structures in sprays. When using POD modes to represent the spray images, a majority of the Total Intensity Fluctuation (TIF) is contained within the first few POD modes. To identify the coherent flow structures caused by the turbulence in the sprays, we study 2 cases of cross sectional fuel spray data with pressure corresponding to 450 bar and 1000 bar.

There are two main objectives in this paper. First, POD is implemented with Matlab and used to analyze cross sectional spray data. Second, the potential of POD in the ICE applications is pointed out to study the mixing quantitatively in turbulent sprays. The organisation of the paper is as follows: In section 2, we study the

*Corresponding author: santosh.tirunagari@aalto.fi

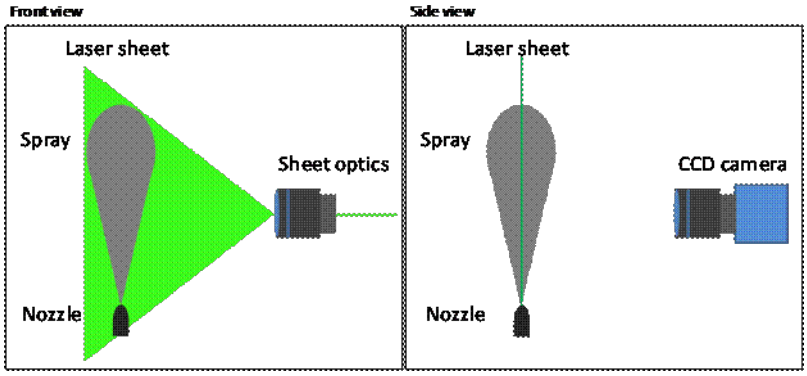

Figure 1. Laser sheet imagining.

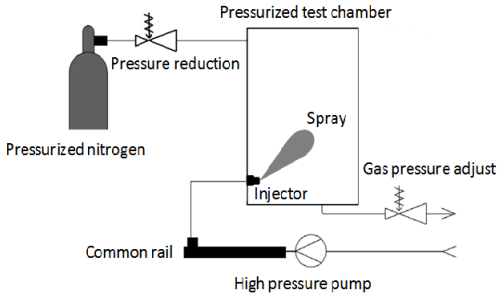

Figure 2. Schematic representation of pressurized test chamber.

experimental methods. Section 3 deals with the implemention details of POD. Results and discussions are made in section 4 and finally, conclusions are drawn and further research directions are discussed in section 5.

Experimental Methods

Experimental fuel spray measurements are performed with laser based sheet imaging system (Figure 1) at pressurized injection test chamber (Figure 2). A slice of the fuel spray is visualized with a thin laser sheet. The intense laser sheet illuminates the droplets on its way through the fuel spray. Scattered light from particles is then recorded with a high-resolution camera. The optical access to the injection test chamber is through four windows at different sides.

The light source is a pulsed Nd:YAG laser sheet with 532 nm wavelength after second harmonic generator. The images are taken with digital monochrome camera (CCD). Duration of a laser pulse is approximately 5 ns. Due to the short light pulse, most motion of high-velocity fuel spray is frozen and high timing accuracy is achieved. The measurements are controlled by a computer, which is also used for data acquisition. The resolution of camera is 2048x2048 pixels (four megapixels) with dynamic range of 12 bit (4096 different levels of grey). The optic is Nikon Micro-Nikkor 105mm teleobjective with 25 mm extension tube. The area of view is approximately 36x36 mm and dimensions of pixel are approximately 17.7x17.7 μm.

The test chamber is imitating physical conditions of diesel engines. However, fuel sprays are non-evaporative and ambient gas density is constant 36 kg/m^3 in the test chamber. Injection pressures are 450 bar and 1000 bar. Maximum variance of injection pressure in common rail is $\pm$25 bar and maximum variance of ambient gas density is $\pm$0.15 kg/m^3. Ambient gas temperature is $20 - 25\ ^\circ C$ when density of ambient gas is kept constant by varying ambient pressure. The pressurizing gas, nitrogen (N2), is flowed continuous through the chamber to ensure that chamber is clear of diesel mist before next injection. The injector is solenoid operated common rail injector. Nozzle orifice diameter is 0.133 mm. The nozzles of this size are commonly used at off-road diesel engine vehicles. The cone angle is 149 degrees. The images are captured 2.500 ms after electric start of injection when injection pressure is 450 bar and 1.830 ms when injection pressure is 1000 bar. Some delay from the electric injection signal to fuel jet exit from the nozzle orifice is occurred. This is mainly due to solenoid operation, needle inertia and fluid inertia. Injected fuel is European standard diesel EN590. Density of fuel is 837.3 kg/m^3 ($15\ ^\circ C$).

Proper Orthogonal Decomposition

POD is first introduced in the field of Computational Fluid Dynamics (CFD) by Lumley [6]. POD is known by various names like Karhunen-Loeve Decomposition (KLD), Principle Componant Analysis (PCA), and Singular Value Decompostion (SVD). It has diversified applications in many fields [7]. This method aims at representing the snapshots (spray images) in terms of orthogonal modes which correspond to the energetic, coherent flow structures. Hence, POD may be used to extract certain derterministic features from turbulent data. POD theory is best described by Chatterjee in [8]. The present day analysis uses method of snapshots introduced by Sirovich [10]. This method is introduced to reduce the POD computations and nowadays this method has become extremely popular [9] [11] [12]. To compute the POD using the original method requires solving $n \times n$ eigenvalue problem, where n is the total number of pixels in a snapshot. The main problem is the calculation of the auto-covariance matrix C. Method of snapshots proposes that the auto-covariance matrix can be approximated by a summation of 'snapshots'. Here U is fluctuating intensity matrix.

$$C_{ij} = \frac{1}{M} \sum_{n=1}^{M} U_i^n U_j^n \tag{1}$$

Implementation of POD

First, the snapshot matrix S is constructed as a part of the POD implementation. Let P_i be the i^{th} spray image whose size is $m \times n$. This image P_i is converted to $mn \times 1$ column vector. Therefore, resulting in the construction of a snapshot matrix S of size $mn \times N$ for N spray images.

$$S = [P^1 P^2 P^3 \cdots P^N] = \begin{pmatrix} P_1^1 & P_1^2 & ... & P_1^N \\ \vdots & \vdots & \vdots & \vdots \\ P_{mn}^1 & P_{mn}^2 & ... & P_{mn}^N \end{pmatrix} \tag{2}$$

The fluctuating intensity matrix U is calculated by substracting the average pixel intensities $\hat{S}$ from the snapshot matrix S,

$$U = S - \hat{S}. \tag{3}$$

The auto-covariance matrix is computed as

$$C = U^T U. \tag{4}$$

An eigenvalue problem for the auto-covariance matrix is then solved

$$CA^i = \lambda^i A^i. \tag{5}$$

The eigenvectors are arranged according to the decreasing order of eigenvalues. This ordering is physically meaningful because, it reflects the fluctuating energies in the POD modes

$$\lambda^1 > \lambda^2 > \lambda^3 > \lambda^4 > \cdots \lambda^N = 0. \tag{6}$$

The relative energies in the eigenvalues are computed as

$$\Xi_i = \frac{\lambda_i}{\sum_{i=1}^{N} \lambda_i}. \tag{7}$$

Using the ordered eigenvectors the POD modes are constructed

$$\phi_i = \frac{\sum_{n=1}^{N} A_n^i U^n}{\| \sum_{n=1}^{N} A_n^i U^n \|}, \qquad i = 1, 2, \cdots, N. \tag{8}$$

POD coefficients are then found projecting the mean centered snapshot matrix onto the POD modes. Each snapshot can be expanded in a series of the POD modes with the expansion coefficients a_i for each mode i

$$a^n = \Psi^T u^n. \tag{9}$$

Here $\Psi = [\phi_1 \phi_2 \cdots \phi_N]$ has been introduced. The expansion of the fluctuating part of the snapshot n is

$$u^n = \sum_{i=1}^{N} a_i^n \phi^i = \Psi a^n \tag{10}$$

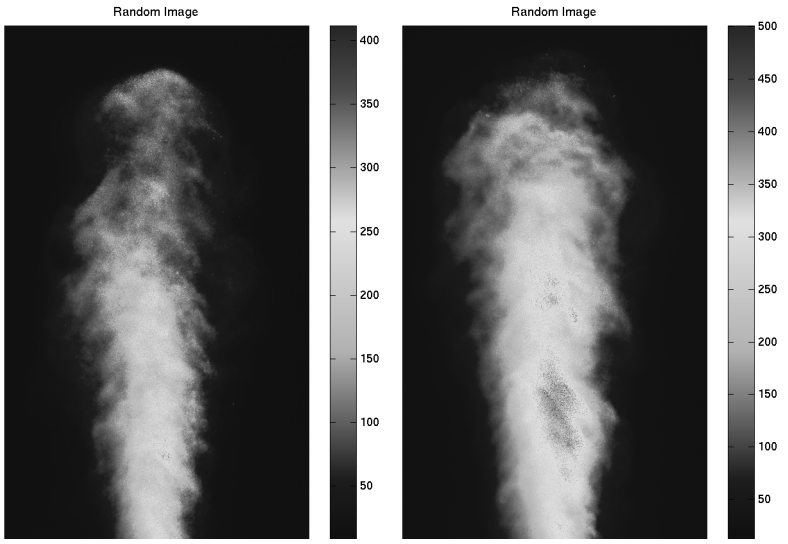

Figure 3. Comparison of random spray snapshots for pressure = 450 bar (left) and pressure = 1000 bar (right).

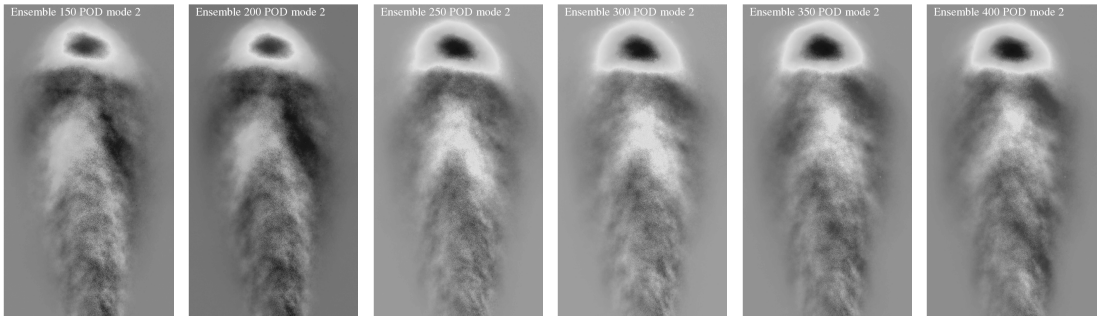

Figure 4. Comparison of POD mode 2 for ensembles 150, 200, 250, 300, 350, 400 corresponding to pressure = 450 bar.

Results and Discussion

A total of 400 spray images are taken for each injection pressures corresponsing to 450 bar and 1000 bar. Figure 3 shows the random spray images for the two injection pressure cases investigated. But only 300 images are analysed with POD considering sensitivity analysis.

Sensitivity Analysis

The sensitivity analysis in this paper reveals that, POD analysis is independent of number of images for considered ensembles. The considered ensembles are of 150, 200, 250, 300, 350, and 400 spray images for each injection pressure case. Figure 4 shows POD mode 2 for injection pressure 450 bar for the different emsembles. It is observed that POD mode 2 for injection pressure 450 bar is qualitatively similar for all ensembles revealing the spray penetration. Figure 5 shows the relative energies for both the pressure cases investigated through sensitivity analysis. Here energy refers to Pixel Intensity Fluctuations (PIF).

For 450 bar pressure case, the energies in the first mode of the ensembles are 55% to 65% and energies from mode 2-10 are around 2% to 3%. For 1000 bar pressure case, the energies in the first mode of the ensembles are 37% to 70% and energies from mode 2-10 are around 2% to 6%. Energy in the eigenvalues depends on the number of snapshots used. Qualitatively the POD modes do not change with respect to number of snapshots used, but the energy fraction do changes. Considering the relative energies, ensemble 300 has a average relative energy fraction compared to other ensembles. Hence ensemble 300 is choosen for this analysis.

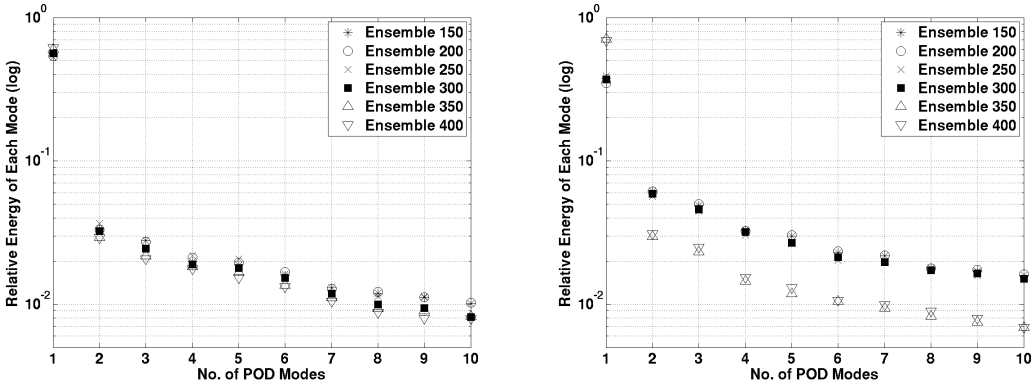

Figure 5. Comparison of energies in POD modes for different ensembles corresponding to pressure = 450 bar (left) and pressure = 1000 bar (right).

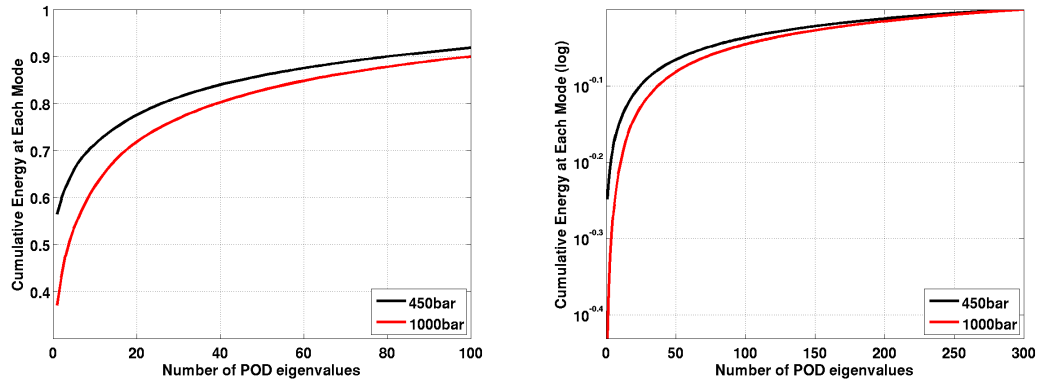

Figure 6. Comparison of cumulative energies of each mode, for pressure = 450 bar and pressure = 1000 bar.

POD Modes

Figure 6 shows the cumulative energies for the pressure cases investigated. 450 bar pressure clearly has more energy when compared to 1000 bar pressure. Only 80 modes are required to capture the 90% of Total Intensity Fluctuations (TIF) for 450 bar injection pressure, where as 100 modes are required to capture 90% of the TIF in the case of 1000 bar injection pressure. The presence of high energy is related to the presence of large scaled structures. These large scaled structures in the POD modes reveal poor mixing. Figure 6, possibly indicates, as the pressure increases, the energy decreases. Hence, decrease in the energy or PIF realize small scale structures. These small scale structures indicate a good mixing proportions in the spray. In other words, as the pressure increases, mixing might get better.

Figure 7 shows the comparison of POD modes for 450 bar pressure (top) and pressure = 1000 bar (bottom). POD mode 1 captures most of the PIF from the spray images and provides extra information over an average image. POD mode 1 shows that, the width and height of the spray for 1000 bar injection pressure is greater than 450 bar injection pressure. It carries 56% of the TIF for injection pressure 450 bar and 37% of the TIF for injection pressure 1000 bar. POD mode 2 reveals a coherent structure with greater intensity fluctuations near the tip region of the spray for both the injection pressures. This phenomenon is due to the spray to spray variations. A tilt in the tip penetration is observed for 1000 bar injection pressure. This possibly indicates a swirl caused in the spray. This swirling structure in the case of 1000 bar injection pressure is captured in POD mode 7. POD mode 2 carries 3% of the TIF for the injection pressure corresponding to 450 bar and 6% of the TIF for the injection pressure corresponding to 1000 bar.

A pair of large scale coherent structures at the tip region are captured in POD mode 3 for both the injection pressures, indicating the spray vortices. Another pair of large scale structures could be observed for 450 bar injection pressure, carrying 2% of the TIF, indicating the presence of Kelvin-Helmholtz instabilies. POD mode 3 carries 3% of the TIF for injection pressure 1000 bar. POD Mode 4 carries 2% and 3% of the TIF for injection

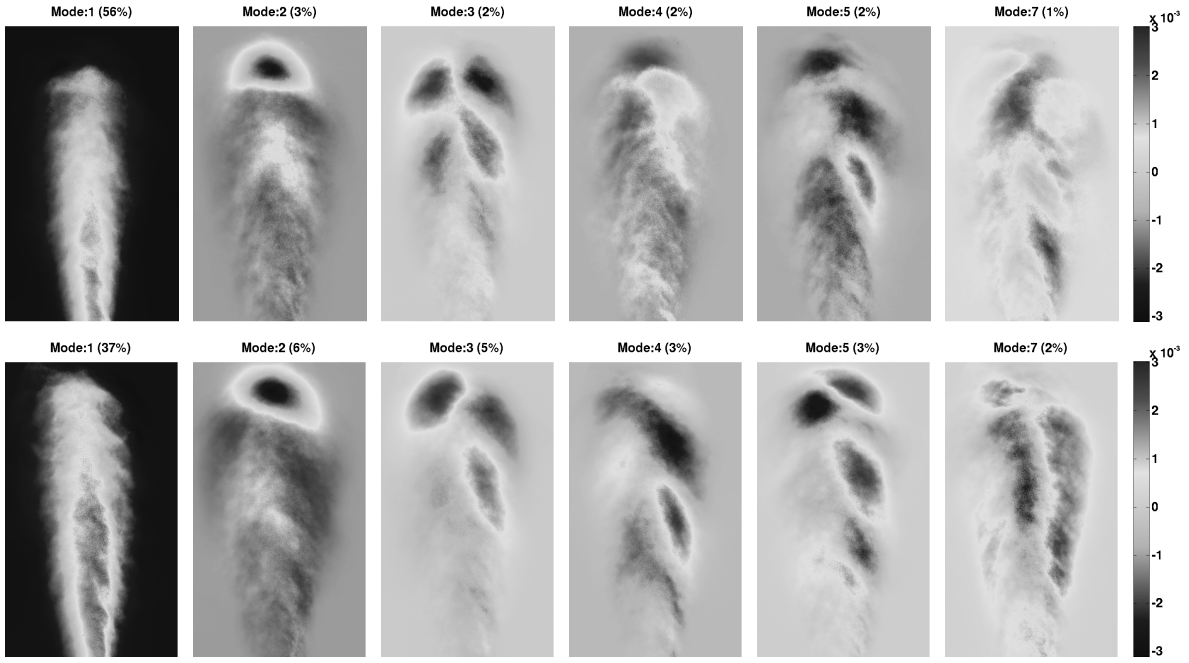

Figure 7. Comparison of POD modes for pressure = 450 bar (top) and pressure = 1000 bar (bottom).

pressure 450 bar and 1000 bar respectively. It reveals tip of the spray, a complementary structure to POD mode 2. POD Mode 5 carries 2% and 3% of the TIF for injection pressures 450 bar and 1000 bar respectively and reveals the formation of the spray vortices, a complementary structure to POD mode 3.

POD Coefficients

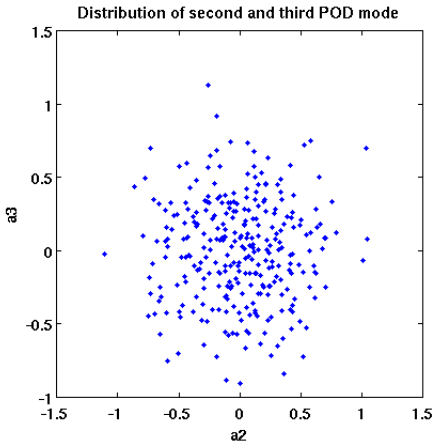

Figure 8. Scatter plot of the POD coefficients for pressure = 450 bar.

POD coefficients are found projecting the mean centered snapshot matrix onto the POD modes. It reveals the inter-connection among the POD modes. Each snapshot can be expanded in a series of the POD modes with the expansion coefficients a_i for each mode i. Figure 8 is the scatterplot of the POD coefficients for POD mode 2 and POD mode 3, showing the relationship between these modes.

- The modes are either symmetric (ring type structures) or anti-symmetric (helical structures) and located in the shear-layer.
- These modes are usually ordered by pair, so plotting a_2 vs a_3 gives a circle or similarly a_2 vs a_4 would give a 8, if a_2 is an harmonic of a_4.

The scatter plot realizes mainly two type of distributions namely, circle (0) or eight (8). The circular distribution reveals a strong connection between the POD modes [11]. In the Figure 8, most of the distribution is pertained to radius 1, from center (a_2,a_3) = (0,0).

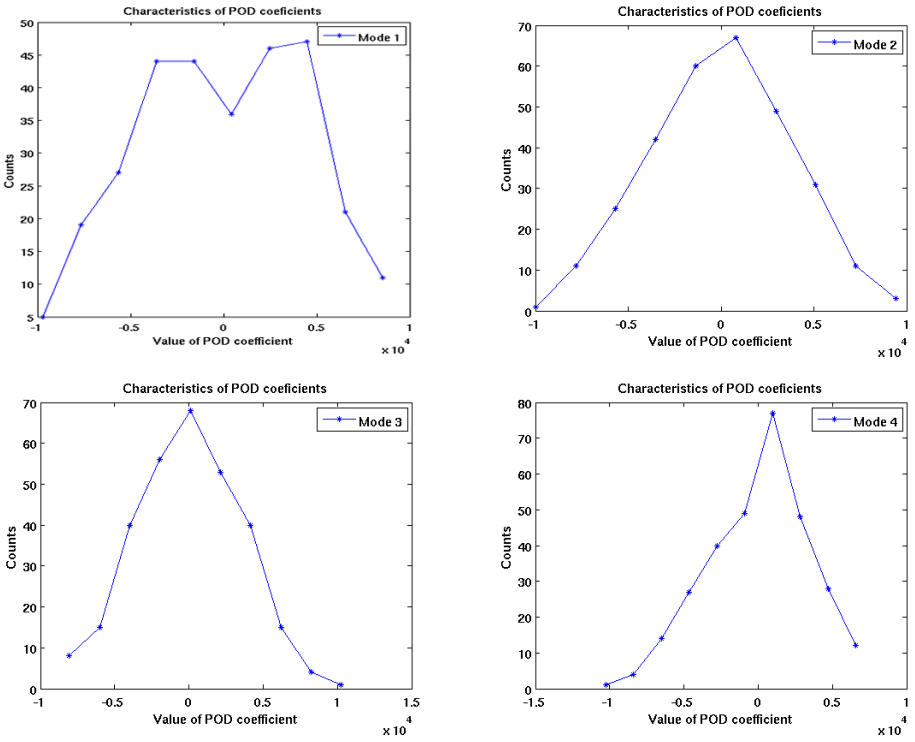

Figure 9. Comparison of first 4 POD mode coefficients for pressure = 450 bar.

The Probability Density Function (PDF) shows certain aspects of the spray structure in Figure 9, which could be speculated as follows: 1) POD mode 1 shows a bimodal distribution possibly indicating the presence of both helical and columnar features instabilities. 2) POD mode 2 and POD mode 3 realize a Gaussian distribution possibly indicating a neutral mode. Hence, the scatterplot of POD coefficients for POD mode 2 and POD mode 3 reveal a circular distribution in Figure 8. 3) POD mode 4 shows a right skewed distribution, possibly indicating the transition in the spray and shift in between the instabilities. Furthermore, it has been found in [13] that PDF's may provide dynamic information on interaction between two modes. For example, Meyer et. al in [11], found that a circular distribution between two POD mode coefficients reveals a strong connection between the POD modes. In our present studies we have not yet found such interactions in a very clear way. For example, in Figure 8 the interaction between POD mode 2 and POD mode 3 looks rather trivial implying that the modes are actually uncorrelated. However, these aspects certainly deserve further attention and the deeper analysis of the PDF's is left to our future studies.

Summary and Conclusions

Cross sectional fuel spray images for injection pressures corresponding to 450 bar and 1000 bar is investigated using POD analysis. These spray images are decomposed into set of orthogonal basis functions using POD, called POD modes. These POD modes are the optimal decomposition for the flow and capture large scale structures thereby providing information on the large scale behaviour. The presence of high TIF is related to the presence of large scaled structures captured in the POD modes. These large scaled structures in the POD modes reveal poor mixing. With the increase in the injection pressure, the TIF is found decreasing. Hence, decrease in the TIF realize small scaled structures. These small scale structures indicate a good mixing proportions in the spray. In other words, as the pressure increases, mixing gets better. Generally 90% of the TIF is used and the average flow field is described in the first few POD modes. The inter-connections among the POD modes is studied using POD coefficients. The power of PODs fast convergence allows for the large scale structures to be isolated from the small scale structures in the turbulence. This would help in analysing the flow field in different ways. The ability to maximize the TIF of the flow with a miminal number of modes shows PODs strength in the analysis of the

coherent flow structures and reduced order modelling.

A characteristic feature of the studied sprays is that it is rather hard to say anything quantitative from the individual spray snapshots. From the snapshots, it actually seems that the spatial distribution of the droplets is rather uniform. Yet, with POD, certain coherent structures from the spatial spray distribution were clearly revealed. In particular, this study established a solid link between the injection pressure and POD energy spectrum. Furthermore, our preliminary studies have in general implied that with basic image processing techniques (filtering, thresholding etc) certain structural aspects on droplet-vortex interaction can be better highlighted from the snapshots. Due to the promising results of the present study, our near-future studies will strongly involve gaining deeper understanding on the effect of injection pressure to mixture quality and droplet-turbulence interactions.

Acknowledgements

The present work is related to the Future Combustion Engine and Powerplant (FCEP) program of the SHOK Cleen Oy. The funding for this work has been provided as a part of FCEP Work Package 1 project. We would like to thank CSC - IT Center for Science Ltd. for providing us with their most powerful supercomputing environment. We would also thank Dr. Christophe Duwig (Lund University) for suggesting sensitivity analysis.

References

[1] Hillamo Harri, “Optical Fuel Spray Measurements“, Doctoral Dissertations 124/2011, Aalto University.

[2] C. Bishop and SpringerLink, ”Pattern recognition and machine learning“. Springer New York, 2006, vol. 4.

[3] R. Perrin, M. Braza, E. Cid, S. Cazin, A. Barthet, A. Sevrain, C. Mockett, and F. Thiele, ”Phase averaged turbulence properties in the near wake of a circular cylinder at high reynolds number using pod”, Experiments in Fluids, vol. 43,pp. 341-355, 2007, 10.1007/s00348-007-0347-6. [Online]. Available:http://dx.doi.org/10.1007/s00348-007-0347-6

[4] K. Meyer, D. Cavar, and J. Pedersen, “Pod as tool for comparison of piv and les data“, in 7th International Symposium on Particle Image Velocimetry, 2007.

[5] Lightfoot, MD and Danczyk, SA and Narayanan, V. and Eilers, B. and Schumaker, SA, ”Use of Proper Orthogonal Decomposition Towards Time-resolved Image Analysis of Sprays”, ILASS Americas, 23rd Annual Conference on Liquid Atomization and Spray Systems, Ventura, CA, May 2011

[6] G. Berkooz, P. Holmes, and J. Lumley, “The proper orthogonal decomposition in the analysis of turbulent flows”, Annual review of fluid mechanics, vol. 25, no. 1, pp. 539-575, 1993.

[7] Mari-Sanna Paukkeri, Ilkka Kivimaki, Santosh Tirunagari, Erkki Oja and Timo Honkela, ”Effect of Dimensionality Reduction on Different Distance Measures in Document Clustering“, Neural Information Processing, Lecture Notes in Computer Science, 2011, Volume 7064/2011, 167-176, DOI: 10.1007/978-3-642-24965-5_19

[8] Chatterjee, A. “An introduction to the proper orthogonal decomposition”, Current Science Vol. 78, No. 7, 2000, pp. 808-817

[9] Chen, H.; Reuss, D. L.; Sick, V. (2011). Analysis of Misfires in a Direct Injection Engine Using Proper-Orthogonal Decomposition". Experiments in Fluids 51(4): 1139-1151.

[10] L. Sirovich, ”Turbulence and the dynamics of coherent structures”. part 1: Coherent structures, Quarterly of applied mathematics, vol. 45, no. 3,pp. 561-571, 1987

[11] Meyer, K.E. and Pedersen, J.M. and Ozcan, O. “A turbulent jet in crossflow analysed with proper orthogonal decomposition“. Journal of Fluid Mechanics, 583 , pp 199-227 DOI:10.1017/S0022112007006143

[12] C. Duwig and P. Iudiciani, “Extended proper orthogonal decomposition for analysis of unsteady flames“, Flow, turbulence and combustion, vol. 84, no. 1, pp. 25-47, 2010

[13] Stephane Roudnitzky, Philippe Druault, Philippe Guibert, ”Proper orthogonal decomposition of in-cylinder engine flow into mean component, coherent structures and random Gaussian fluctuations“, Journal of Turbulence, Vol. 7, 2009